THE JOURNAL OF BIOLOGICAL CHEMISTRY
Vol. 275, No. 6, Issue of February 11, pp. 3896–3906, 2000

Printed in U.S.A.

Biosynthesis of Ganglioside Mimics in *Campylobacter jejuni* OH4384

IDENTIFICATION OF THE GLYCOSYLTRANSFERASE GENES, ENZYMATIC SYNTHESIS OF MODEL COMPOUNDS, AND CHARACTERIZATION OF NANOMOLE AMOUNTS BY 600-MHz ^{1}H AND ^{13}C NMR ANALYSIS*

(Received for publication, May 28, 1999, and in revised form, October 27, 1999)

Michel Gilbert, Jean-Robert Brisson, Marie-France Karwaski, Joseph Michniewicz, Anna-Maria Cunningham, Yuyang Wu, N. Martin Young, and Warren W. Wakarchuk‡

From the Institute for Biological Sciences, National Research Council of Canada, Ottawa, Ontario K1A 0R6, Canada

We have applied two strategies for the cloning of four genes responsible for the biosynthesis of the GT1a ganglioside mimic in the lipooligosaccharide (LOS) of a bacterial pathogen, *Campylobacter jejuni* OH4384, which has been associated with Guillain-Barré syndrome. We first cloned a gene encoding an α-2,3-sialyltransferase (*cst-I*) using an activity screening strategy. We then used nucleotide sequence information from the recently completed sequence from *C. jejuni* NCTC 11168 to amplify a region involved in LOS biosynthesis from *C. jejuni* OH4384. The LOS biosynthesis locus from *C. jejuni* OH4384 is 11.47 kilobase pairs and encodes 13 partial or complete open reading frames, while the corresponding locus in *C. jejuni* NCTC 11168 spans 13.49 kilobase pairs and contains 15 open reading frames, indicating a different organization between these two strains. Potential glycosyltransferase genes were cloned individually, expressed in *Escherichia coli*, and assayed using synthetic fluorescent oligosaccharides as acceptors. We identified genes encoding a β-1,4-*N*-acetylgalactosaminyl-transferase (*cgtA*), a β-1,3-galactosyltransferase (*cgtB*), and a bifunctional sialyltransferase (*cst-II*), which transfers sialic acid to O-3 of galactose and to O-8 of a sialic acid that is linked α-2,3- to a galactose. The linkage specificity of each identified glycosyltransferase was confirmed by NMR analysis at 600 MHz on nanomole amounts of model compounds synthesized *in vitro*. Using a gradient inverse broadband nano-NMR probe, sequence information could be obtained by detection of ^{3}J(C,H) correlations across the glycosidic bond. The role of *cgtA* and *cst-II* in the synthesis of the GT1a mimic in *C. jejuni* OH4384 were confirmed by comparing their sequence and activity with corresponding homologues in two related *C. jejuni* strains that express shorter ganglioside mimics in their LOS.

Since the late 1970s, *Campylobacter jejuni* has been recognized as an important cause of acute gastroenteritis in humans (1). Epidemiological studies have shown that *Campylobacter* infections are more common in developed countries than *Salmonella* infections, and they are also an important cause of diarrheal diseases in developing countries (2). In addition to causing acute gastroenteritis, *C. jejuni* infection has been implicated as a frequent antecedent to the development of Guillain-Barré syndrome, a form of neuropathy that is the most common cause of generalized paralysis (3). One of the most common *C. jejuni* serotypes associated with Guillain-Barré syndrome is O:19 (4), and this prompted detailed study of the LOS structure of strains belonging to this serotype, including strains OH4382 and OH4384, which were isolated from two siblings who developed the Guillain-Barré syndrome (5–8). The core oligosaccharides of low molecular weight LOS[1] of O:19 strains were shown to exhibit molecular mimicry of gangliosides (Fig. 1). Terminal oligosaccharide moieties identical to those of GM1, GD1a, GD3, and GT1a[2] gangliosides have been found in various O:19 strains. The most extensive structure, a trisialylated ganglioside mimic of GT1a, has been observed in the strain OH4384. Molecular mimicry of host structures by the saccharide portion of LOS is considered to be a virulence factor of various mucosal pathogens, which could use this strategy to evade the immune response (9, 10). Consequently, the identification of the genes involved in LOS synthesis and the study of their regulation is of considerable interest for a better understanding of the pathogenesis mechanisms used by these bacteria.

The cloning and characterization of a gene (heptosyltransferase I) involved in the synthesis of the LOS inner core has been reported (11), while two other groups (12, 13) have reported the cloning of LPS biosynthesis genes. Some of these genes are homologous to bacterial glycosyltransferases, but none have been linked unequivocally to the synthesis of the LOS outer core. The genes reported by Fry *et al*. (12) and Wood *et al*. (13) could be involved in the synthesis of the O-chain or in the synthesis of another cell-associated carbohydrate. Recently, the genome sequence of the *C. jejuni* strain NCTC 11168 has been completed by the Sanger Centre. The serotype of this strain is O:2, but its core oligosaccharide structure is not known. This genome sequence therefore represents a source of

* The costs of publication of this article were defrayed in part by the payment of page charges. This article must therefore be hereby marked "*advertisement*" in accordance with 18 U.S.C. Section 1734 solely to indicate this fact.

The nucleotide sequences reported in this paper have been submitted to GenBank™/EBI Data Bank with the accession numbers AF130466, AF130984, and AF167345.

‡ To whom correspondence should be addressed: Inst. for Biological Sciences, National Research Council of Canada, 100 Sussex Dr., Ottawa, Ontario K1A 0R6, Canada. Tel.: 613-990-0817; Fax: 613-941-1327; E-mail: warren.wakarchuk@nrc.ca.

[1] The abbreviations used are: LOS, lipooligosaccharide; CMP-Neu5Ac, cytidine monophosphate-*N*-acetylneuraminic acid; COSY, correlated spectroscopy; FCHASE, 6-(5-fluorescein-carboxamido)-hexanoic acid succimidyl ester; HMBC, heteronuclear multiple bond coherence; HSQC, heteronuclear single quantum coherence; LPS, lipopolysaccharide; NOE, nuclear Overhauser effect; NOESY, NOE spectroscopy; TOCSY, total correlation spectroscopy; aa, amino acid(s); kb, kilobase pair(s); ORF, open reading frame; PCR, polymerase chain reaction; Mops, 4-morpholinepropanesulfonic acid; Mes, 4-morpholineethanesulfonic acid; IPTG, isopropyl-1-thio-β-D-galactopyranoside; MALDI-TOF, matrix-assisted laser desorption ionization/time of flight.

[2] The abbreviated designations of glycolipids are according to IUPAC-IUC nomenclature (see Ref. 31).

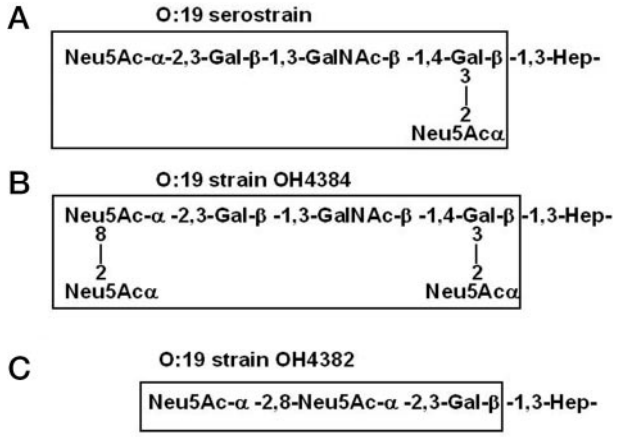

FIG. 1. **LOS outer core structures from *C. jejuni* O:19 strains.** These structures were determined by Aspinall *et al.* (6), and the portions showing similarity with the oligosaccharide portion of gangliosides are delimited by *boxes*. *A*, *C. jejuni* O:19 serostrain (ATCC 43446) showing structural similarity with the oligosaccharide portion of ganglioside GD1a. *B*, *C. jejuni* OH4384 showing structural similarity with the oligosaccharide portion of ganglioside GT1a. *C*, *C. jejuni* OH4382 showing structural similarity with the oligosaccharide portion of ganglioside GD3.

information for the identification of the genes involved in the synthesis of the outer core of the LOS.

In addition to their importance for pathogenesis studies, bacterial glycosyltransferases have been shown to be tools for the chemo-enzymatic syntheses of oligosaccharides with biological activity (14, 15). Since many bacterial glycosyltransferases catalyze the formation of oligosaccharides identical to mammalian structures and they are easier to produce in quantity (15, 16), they are attractive alternatives to the equivalent mammalian glycosyltransferases. The ganglioside mimics synthesized by many *C. jejuni* O:19 strains contain α-2,3- and α-2,8-linked sialic acids; this organism is then a source of both α-2,3- and α-2,8- sialyltransferases.

In this work, we report the sequencing of a locus involved in the biosynthesis of the LOS outer core and the cloning and expression of four glycosyltransferases, which encode enzyme activities required for the biosynthesis of ganglioside mimics by *C. jejuni* OH4384, which has been implicated in Guillain-Barré syndrome. One of these enzymes is a novel bifunctional sialyltransferase, which makes both α-2,3 and α-2,8-sialic acid linkages. The ^{1}H and ^{13}C NMR analysis was done on nanomole amounts of enzymatic product using homonuclear and heteronuclear methods. For one compound, the α-2,3 and α-2,8-sialic acid linkages were confirmed by using a gradient inverse broadband nano-NMR probe to detect the $^{3}J(C,H)$ correlation across the glycosidic bonds.

EXPERIMENTAL PROCEDURES

Bacterial Strains—The following *C. jejuni* strains were used in this study: serostrain O:19 (ATCC 43446); serotype O:19, strains OH4382 and OH4384 were obtained from the Laboratory Center for Disease Control (Health Canada, Winnipeg, Manitoba, Canada); and serotype O:2 (NCTC 11168). *Escherichia coli* DH5α was used for the *Hin*dIII library, while *E. coli* AD202 (CGSG 7297) was used to express the different cloned glycosyltransferases.

Basic Recombinant DNA Method—Genomic DNA isolation from the *C. jejuni* strains was performed using Qiagen Genomic-tip 500/G (Qiagen Inc., Valencia, CA). Plasmid DNA isolation, restriction enzyme digestions, purification of DNA fragments for cloning, ligations, and transformations were performed as recommended by the enzyme supplier, or the manufacturer of the kit used for the particular procedure. Long PCR reactions (>3 kb) were performed using the Expand™ long template PCR system as described by the manufacturer (Roche Molecular Biochemicals). PCR reactions to amplify specific open reading frames (ORFs) were performed using the *Pwo* DNA polymerase as described by the manufacturer (Roche Molecular Biochemicals). Restriction and DNA modification enzymes were purchased from New England Biolabs Ltd. (Mississauga, Ontario, Canada). DNA sequencing was performed using an Applied Biosystems (Montreal, Quebec, Canada) model 370A automated DNA sequencer and the manufacturer's cycle sequencing kit.

Activity Screening for Sialyltransferase from C. jejuni—The genomic library was prepared using a partial *Hin*dIII digest of the chromosomal DNA of *C. jejuni* OH4384. The partial digest was purified on a QIAquick column (QIAGEN Inc.) and ligated with *Hin*dIII-digested pBluescript SK−. *E. coli* DH5α was electroporated with the ligation mixture and the cells were plated on LB medium with 150 μg/ml ampicillin, 0.05 mM IPTG, and 100 μg/ml 5-bromo-4-chloro-indolyl-β-D-galactopyranoside. White colonies were picked in pools of 100 and were resuspended in 1 ml of medium with 15% glycerol. Twenty μl of each pool were used to inoculate 1.5 ml of LB medium supplemented with 150 μg/ml ampicillin. After 2 h of growth at 37 °C, IPTG was added to 1 mM and the cultures were grown for another 4.5 h. The cells were recovered by centrifugation, resuspended in 0.5 ml of 50 mM Mops (pH 7, 10 mM $MgCl_2$) and sonicated for 1 min. The extracts were assayed for sialyltransferase activity as described below, except that the incubation time and temperature were 18 h and 32 °C, respectively. The positive pools were plated for single colonies, and 200 colonies were picked and tested for activity in pools of 10. Finally the colonies of the positive pools were tested individually, which led to the isolation of a two positive clones, pCJH9 (5.3-kb insert) and pCJH101 (3.9-kb insert). Using several subcloned fragments and custom-made primers, the inserts of the two clones were completely sequenced on both strands. The clones with individual *Hin*dIII fragments were also tested for sialyltransferase activity, and the insert of the only positive one (a 1.1-kb Hind*III* fragment cloned in pBluescript SK−) was transferred to pUC118 using *Kpn*I and *Pst*I sites in order to obtain the insert in the opposite orientation with respect to the *plac* promoter.

Cloning and Sequencing of an LOS Biosynthesis Locus—The primers used to amplify the LOS biosynthesis locus of *C. jejuni* OH4384 were based on preliminary sequences from the complete genome of the strain NCTC 11168 (available via the World Wide Web from the Sanger Center). The primers CJ-42 (5′-GCCATTACCGTATCGCCTAACCAGG-3′; 25-mer) and CJ-43 (5′-AAAGAATACGAATTTGCTAAAGAGG-3′; 25-mer) were used to amplify an 11.47-kb locus using the Expand™ long template PCR system. The PCR product was purified on a S-300 spin column (Amersham Pharmacia Biotech) and completely sequenced on both strands using a combination of primer walking and subcloning of *Hin*dIII fragments. Specific ORFs were amplified using the *Pwo* DNA polymerase. The PCR products were digested using the appropriate restriction enzymes and were cloned in the expression vector pCWori+ (17).

Assays—Protein concentration was determined using the bicinchoninic acid protein assay kit (Pierce). For all of the enzymatic assays, 1 unit of activity was defined as the amount of enzyme that generated 1 μmol of product/min. FCHASE-labeled oligosaccharides were prepared as described previously (18). The screening assay for α-2,3-sialyltransferase activity in pools of clones contained 1 mM Lac-FCHASE, 0.2 mM CMP-Neu5Ac, 50 mM Mops, pH 7, 10 mM $MnCl_2$, and 10 mM $MgCl_2$ in a final volume of 10 μl. The various subcloned ORFs were tested for the expression of glycosyltransferase activities following a 4-h induction of the cultures with 1 mM IPTG. Extracts were made by sonication and the enzymatic reactions were performed overnight at 32 °C. The β-1,3-galactosyltransferase was assayed using 0.2 mM GM2-FCHASE (a generous gift of Dr. Eric Sjoberg, Cytel Corp.), 1 mM UDP-Gal, 50 mM Mes, pH 6, 10 mM $MnCl_2$, and 1 mM dithiothreitol. The β-1,4-GalNAc transferase was assayed using 0.5 mM GM3-FCHASE, 1 mM UDP-GalNAc, 50 mM Hepes, pH 7, and 10 mM $MnCl_2$. The α-2,3-sialyltransferase was assayed using 0.5 mM Lac-FCHASE, 0.2 mM CMP-Neu5Ac, 50 mM Hepes, pH 7, and 10 mM $MgCl_2$. The α-2,8-sialyltransferase was assayed using 0.5 mM GM3-FCHASE, 0.2 mM CMP-Neu5Ac, 50 mM Hepes, pH 7, and 10 mM $MnCl_2$. The reaction mixes were diluted appropriately with 10 mM NaOH and analyzed by capillary electrophoresis performed using the separation and detection conditions as described previously (19). The peaks from the electropherograms were analyzed using manual peak integration with the P/ACE Station software. For rapid detection of enzyme activity, samples from the transferase reaction mixtures were examined by thin layer chromatography on Silica-60 TLC plates (Merck) as described previously (19).

NMR Spectroscopy—NMR experiments were performed on a Varian INOVA 600 NMR spectrometer. Most experiments were done using a 5-mm Z gradient triple resonance probe. NMR samples were prepared

from 0.3 to 0.5 mg (200–500 nmol) of FCHASE-glycoside. The compounds were dissolved in H_2O, and the pH was adjusted to 7.0 with dilute NaOH. After freeze-drying, the samples were dissolved in 600 μl of D_2O. All NMR experiments were performed as described previously (20, 21) using standard techniques such as COSY, TOCSY, NOESY, one-dimensional NOESY, one-dimensional TOCSY, and HSQC. For the proton chemical shift reference, the methyl resonance of internal acetone was set at 2.225 ppm (^{1}H). For the ^{13}C chemical shift reference, the methyl resonance of internal acetone was set at 31.07 ppm relative to external dioxane at 67.40 ppm. Homonuclear experiments were on the order of 5–8 h each. The one-dimensional NOESY experiments for GD3-FCHASE (0.3 mM), with 8000 scans and a mixing time of 800 ms was done for a duration of 8.5 h each and processed with a line broadening factor of 2–5 Hz. For the one-dimensional NOESY of the resonances at 4.16 ppm, 3000 scans were used. The following parameters were used to acquire the HSQC spectrum: relaxation delay of 1.0 s, spectral widths in F_2 and F_1 of 6000 and 24147 Hz, respectively, acquisition times in t_2 of 171 ms. For the t_1 dimension, 128 complex points were acquired using 256 scans/increment. The sign discrimination in F_1 was achieved by the States method. The total acquisition time was 20 h. For GM2-FCHASE, due to broad lines, the number of scans per increment was increased so that the HSQC was performed for 64 h. The phase-sensitive spectrum was obtained after zero filling to 2048 $\times$ 2048 points. Unshifted gaussian window functions were applied in both dimensions. The HSQC spectra were plotted at a resolution of 23 Hz/point in the ^{13}C dimension and 8 Hz/point in the proton dimension. For the observation of the multiplet splittings, the ^{1}H dimension was reprocessed at a resolution of 2 Hz/point using forward linear prediction and a π/4-shifted squared sinebell function. All the NMR data were acquired using Varian's standard sequences provided with the VNMR 5.1 or VNMR 6.1 software. The same program was used for processing.

A gradient inverse broadband nano-NMR probe (Varian) was used to perform the gradient HMBC (22, 23) experiment for the GD3-FCHASE sample. The nano-NMR probe, which is a high resolution, magic angle spinning probe, produces high resolution spectra of liquid samples dissolved in only 40 μl (24). The GD3-FCHASE sample (mass = 1486.33 Da) was prepared by lyophilizing the original 0.6-ml sample (200 nmol) and dissolving it in 40 μl of D_2O for a final concentration of 5 mM. The final pH of the sample could not be measured. The gradient HMBC experiment was done at a spin rate of 2990 Hz, 400 increments of 1024 complex points, 128 scans per increment, acquisition time of 0.21 s, ^{1}J(C,H) = 140 Hz, and ^{n}J(C,H) = 8 Hz, for a duration of 18.5 h.

Mass Spectrometry—All mass measurements were obtained using a Perkin-Elmer Biosystems (Fragmingham, MA) Elite-STR MALDI-TOF instrument. Approximately 2 μg of each oligosaccharide was mixed with a matrix containing a saturated solution of dihydroxybenzoic acid. Positive and negative mass spectra were acquired using the reflector mode.

RESULTS

Detection of Glycosyltransferase Activities in C. jejuni Strains—Before the cloning of the glycosyltransferases, we examined *C. jejuni* OH4384 and NCTC 11168 cells for various enzymatic activities. When an enzyme activity was detected, we then optimized the assay conditions (described under "Experimental Procedures") to ensure maximal activity. The capillary electrophoresis assay we employed was extremely sensitive and allowed detection of enzyme activity in the microunits/ml range (19). We examined both the sequenced strain NCTC 11168 and the Guillain-Barré syndrome åssociated strain OH4384 for the enzymes required for the GT1a ganglioside mimic synthesis. As predicted, strain OH4384 possessed the enzyme activities required for the synthesis of this structure: β-1,4-*N*-acetylgalactosaminyltransferase, β-1,3-galactosyltransferase, α-2,3-sialyltransferase, and α-2,8-sialyltransferase. The genome strain, NCTC 11168, lacked the β-1,3-galactosyltransferase and the α-2,8-sialyltransferase activities. Since the LOS structure for NCTC 11168 has not yet been reported, we do not yet know if the presence or absence of a particular enzyme activity in this strain correlates with the structure of its LOS outer core oligosaccharide.

Cloning of an α-2,3-Sialyltransferase (cst-I) Using an Activity Screening Strategy—A plasmid library made from an unfractionated partial *Hin*dIII digestion of chromosomal DNA from *C. jejuni* OH4384 yielded 2,600 white colonies which were picked to form pools of 100. We used a "divide and conquer" screening protocol from which two positive clones were obtained and designated pCJH9 (5.3-kb insert, 3 *Hin*dIII sites) and pCJH101 (3.9-kb insert, 4 *Hin*dIII sites). ORF analysis and PCR reactions with *C. jejuni* OH4384 chromosomal DNA (data not shown) indicated that pCJH9 contained inserts that were not contiguous in the chromosomal DNA. The sequence downstream of nucleotide 1440 in pCJH9 was not further studied, while the first 1439 nucleotides were found to be completely contained within the sequence of pCJH101. The ORF analysis and PCR reactions with chromosomal DNA indicated that all of the pCJH101 *Hin*dIII fragments were contiguous in *C. jejuni* OH4384 chromosomal DNA.

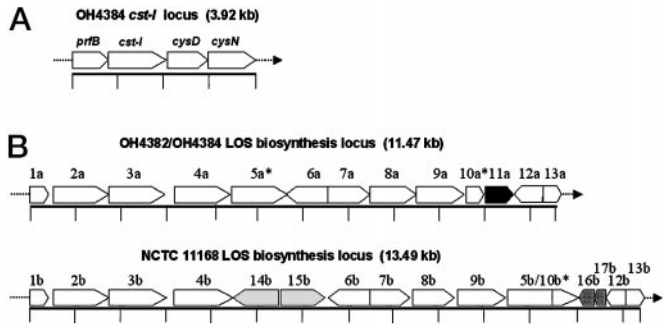

FIG. 2. **Genetic organization of the *cst-I* locus from OH4384 and comparison of the LOS biosynthesis loci from OH4384 and NCTC 11168.** The distance between the scale marks is 1 kb. *A*, the nucleotide sequence of the OH4384 *cst-I* locus is available from GenBank (accession no. AF130466). The partial *prfB* gene is homologous to a peptide chain release factor (GenBank accession no. AE000537) from *H. pylori*, while the *cysD* gene and the partial *cysN* gene are homologous to *E. coli* genes encoding sulfate adenylyltransferase subunits (GenBank accession no. AE000358). *B*, the nucleotide sequence of the OH4384 LOS biosynthesis locus is available from GenBank (accession no. AF130984). The sequence of the OH4382 LOS biosynthesis locus is identical to OH4384, except for the *cgtA* gene, which misses an "A" (see text and GenBank accession no. AF167345). The sequence of the NCTC 11168 LOS biosynthesis locus is available from the Sanger Centre via the World Wide Web. Corresponding homologous genes have the same number with a trailing "a" for the OH4384 genes and a trailing "b" for the NCTC 11168 genes. A gene unique to the OH4384 strain is shown in *black*, and genes unique to NCTC 11168 are shown in *gray*. The OH4384 ORFs 5a and 10a are found as an in-frame fusion ORF (5b/10b) in NCTC 11168 and are denoted with an *asterisk* (*). Proposed functions for each ORF are found in Table II.

Four ORFs, two partial and two complete, were found in the sequence of pCJH101 (Fig. 2). The first 812 nucleotides encode a polypeptide that is 69% identical with the last 265 amino acid (aa) residues of the peptide chain release factor RF-2 (*prfB* gene, GenBank AE000537) from *Helicobacter pylori*. The last base of the TAA stop codon of the chain release factor is also the first base of the ATG start codon of an open reading frame that spans nucleotides 812–2104 in pCJH101. This ORF was designated *cst-I* (*Campylobacter* sialyltransferase I) and encodes a 430-aa polypeptide that is homologous with a putative ORF from *Haemophilus influenzae* (GenBank accession no. U32720). The putative *H. influenzae* ORF encodes a 231-aa polypeptide that is 39% identical to the middle region of the Cst-I polypeptide (aa residues 80–330). The sequence downstream of *cst-I* includes an ORF and a partial ORF that encode polypeptides that are homologous (>60% identical) with the two subunits, CysD and CysN, of the *E. coli* sulfate adenylyltransferase (GenBank accession no. AE000358).

In order to confirm that the *cst-I* ORF encodes sialyltransferase activity, we subcloned it and overexpressed it in *E. coli*. The expressed enzyme was used to add sialic acid to Gal-β-1,4-Glc-β-FCHASE (Lac-FCHASE). This product (GM3-FCHASE) was analyzed by NMR to confirm the Neu5Ac-α-2,3-Gal linkage

TABLE I
Proton NMR chemical shifts for the fluorescent derivatives of the ganglioside mimics synthesized using the cloned glycosyltransferases

Residue	Chemical shift (ppm)[a]					
	H	Lac-	GM3-	GM2-	GM1a-	GD3-
βGlc (a)	1	4.57	4.70	4.73	4.76	4.76
	2	3.23	3.32	3.27	3.30	3.38
	3	3.47	3.54	3.56	3.58	3.57
	4	3.37	3.48	3.39	3.43	3.56
	5	3.30	3.44	3.44	3.46	3.50
	6	3.73	3.81	3.80	3.81	3.85
	6′	3.22	3.38	3.26	3.35	3.50
βGal(1–4) (b)	1	4.32	4.43	4.42	4.44	4.46
	2	3.59	3.60	3.39	3.39	3.60
	3	3.69	4.13	4.18	4.18	4.10
	4	3.97	3.99	4.17	4.17	4.00
	5	3.81	3.77	3.84	3.83	3.78
	6	3.86	3.81	3.79	3.78	3.78
	6′	3.81	3.78	3.79	3.78	3.78
αNeu5Ac(2–3) (c)	3_{ax}		1.81	1.97	1.96	1.78
	3_{eq}		2.76	2.67	2.68	2.67
	4		3.69	3.78	3.79	3.60
	5		3.86	3.84	3.83	3.82
	6		3.65	3.49	3.51	3.68
	7		3.59	3.61	3.60	3.87
	8		3.91	3.77	3.77	4.15
	9		3.88	3.90	3.89	4.18
	9′		3.65	3.63	3.64	3.74
	NAc		2.03	2.04	2.03	2.07
βGalNAc(1–4) (d)	1			4.77	4.81	
	2			3.94	4.07	
	3			3.70	3.82	
	4			3.93	4.18	
	5			3.74	3.75	
	6			3.86	3.84	
	6′			3.86	3.84	
	NAc			2.04	2.04	
βGal(1–3) (e)	1				4.55	
	2				3.53	
	3				3.64	
	4				3.92	
	5				3.69	
	6				3.78	
	6′				3.74	
αNeu5Ac(2–8) (f)	3_{ax}					1.75
	3_{eq}					2.76
	4					3.66
	5					3.82
	6					3.61
	7					3.58
	8					3.91
	9					3.88
	9′					3.64
	NAc					2.02

[a] Proton NMR chemical shifts are given in ppm from HSQC spectrum obtained at 600 MHz, D_2O, pH 7, 28 °C for Lac-, 25 °C for GM3-, 16 °C for GM2-, 24 °C for GM1a-, and 24 °C GD3-FCHASE. The methyl resonance of internal acetone is at 2.225 ppm (^{1}H). The error is ±0.02 ppm for ^{1}H chemical shifts and ±5 °C for the sample temperature. The error is ±0.1 ppm for the H-6 resonances of residues a, b, d, and e due to overlap.

specificity of Cst-I (see text below, Table I, and Figs. 3 and 5).

Sequencing of the LOS Biosynthesis Locus of C. jejuni OH4384—Analysis of the sequence data available at the website of the *C. jejuni* NCTC 11168 sequencing group (Sanger Centre) revealed that the two heptosyltransferases involved in the synthesis of the inner core of the LPS were readily identifiable by sequence homology with other bacterial heptosyltransferases. The region between the two heptosyltransferases spans 13.49 kb in NCTC 11168 and includes at least seven potential glycosyltransferases based on BLAST searches in GenBank. Since no structure is available for the LOS outer core of NCTC 11168, it was impossible to suggest functions for the putative glycosyltransferase genes in that strain.

Based on conserved regions in the heptosyltransferases sequences, we designed primers (CJ-42 and CJ-43) to amplify the region between them. We obtained a PCR product of 13.49 kb using chromosomal DNA from *C. jejuni* NCTC 11168 and a PCR product of 11.47 kb using chromosomal DNA from *C. jejuni* OH4384. The size of the PCR product from strain NCTC 11168 was consistent with the Sanger Center data. The smaller size of the PCR product from strain OH4384 indicated heterogeneity between the strains in the region between the two heptosyltransferase genes and suggested that the genes for some of the glycosyltransferases specific to strain OH4384 could be present in that location. We sequenced the 11.47-kb PCR product using a combination of primer walking and subcloning of *Hin*dIII fragments (GenBank accession no. AF130984). The G/C content of the DNA was 27%, typical of DNA from *Campylobacter*. Analysis of the sequence suggests the presence of 11 complete ORFs in addition to the two partial ORFs encoding the two heptosyltransferases (Fig. 2, Table II). When comparing the deduced amino acid sequences, we found that the two strains share six genes that are above 80% identical and four genes that are between 52 and 68% identical (Table II). Four genes are unique to *C. jejuni* NCTC 11168, while one gene is unique to *C. jejuni* OH4384 (Fig. 2). Two genes that are present as separate ORFs (ORFs 5a and 10a) in *C. jejuni* OH4384 are found in an in-frame fusion ORF (5b/10b) in *C. jejuni* NCTC 11168.

Identification of Outer Core Glycosyltransferases—Various constructs were made to express each of the potential glycosyltransferase genes located between the two heptosyltransferases from *C. jejuni* OH4384. The plasmid pCJL-09 contained the ORF 5a, and a culture of this construct showed GalNAc transferase activity when assayed using GM3-FCHASE as acceptor. The GalNAc transferase was specific for a sialylated acceptor since Lac-FCHASE was a poor substrate (less than 2% of the activity observed with GM3-FCHASE). The reaction product obtained from GM3-FCHASE had the correct mass, as determined by MALDI-TOF mass spectrometry, and an elution time in the capillary electrophoresis assay identical to that for the GM2-FCHASE standard. Considering the structure of the outer core LPS of *C. jejuni* OH4384, this GalNAc transferase (*cgtA* for *Campylobacter* glycosyltransferase A), has a β-1,4-specificity to the terminal Gal residue of GM3-FCHASE. The linkage specificity of CgtA was confirmed by the NMR analysis of GM2-FCHASE (see text below, Table I, and Figs. 3 and 5). The *in vivo* role of *cgtA* in the synthesis of a GM2 mimic is confirmed by the natural knock-out mutant provided by *C. jejuni* OH4382 (Fig. 1). Upon sequencing of the *cgtA* homologue from *C. jejuni* OH4382 we found a frameshift mutation (a stretch of seven A nucleotides instead of 8 A nucleotides after base 71), which would result in the expression of a truncated cgtA version (29 instead of 347 aa). The LOS outer core structure of *C. jejuni* OH4382 is consistent with the absence of β-1,4-GalN transferase as the inner galactose residue is substituted with sialic acid only (6).

The plasmid pCJL-04 contained the ORF 6a and an IPTG-induced culture of this construct showed galactosyltransferase activity using GM2-FCHASE as an acceptor thereby producing GM1a-FCHASE. This product was sensitive to β-1,3-galactosidase and was found to have the correct mass by MALDI-TOF mass spectrometry. Considering the structure of the LOS outer core of *C. jejuni* OH4384, we suggest that this galactosyltransferase (*cgtB* for *Campylobacter* glycosyltransferase B), has β-1,3- specificity to the terminal GalNAc residue of GM2-

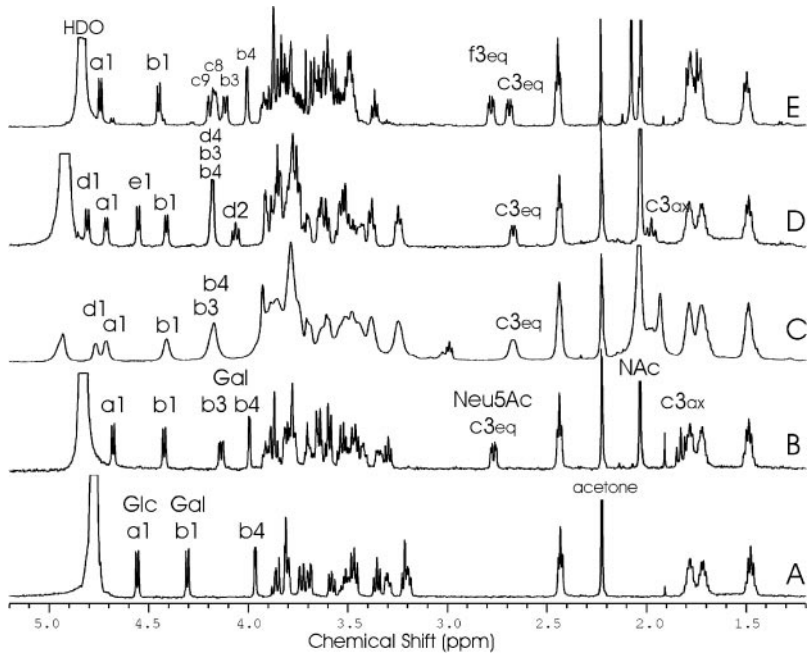

FIG. 3. **Proton one-dimensional NMR spectra at 600 MHz of FCHASE-glycosides.** *A*, Lac- at 25 °C with 16 scans; *B*, GM3- at 20 °C with 16 scans; *C*, GM2 at 12 °C with 256 scans and HDO presaturated; *D*, GM1a- at 12 °C with 16 scans; and *E*, GD3- at 20 °C with 16 scans. The acetone peak is set at 2.225 ppm. The HDO peak is at 4.92 ppm for 12 °C, 4.83 ppm for 20 °C, and 4.77 ppm for 25 °C. All data were processed with a line broadening factor of 1 Hz. Peaks are labeled using *a* for Glc, *b* for Gal(1–4), *c* for Neu5Ac(2–3), *d* for GalNAc(1–4), *e* for Gal(1–3), and *f* for Neu5Ac(2–8), and by the atom number as in Tables I and III.

TABLE II
Location and description of the ORFs of the LOS biosynthesis locus from C. jejuni OH4384

ORF no.	Location	Homologue in strain NCTC11168[a] (% identity in the aa sequence)	Homologues found in GenBank (GB) (% identity in the aa sequence)	Proposed function[b]
1a	1–357	ORF 1b (98%)	*rfaC* (GB AE000546) from *H. pylori* (35%)	Heptosyltransferase I
2a	350–1,234	ORF 2b (96%)	*waaM* (GB AE001463) from *H. pylori* (25%)	Lipid A biosynthesis acyltransferase
3a	1,234–2,487	ORF 3b (90%)	*lgtF* (GB U58765) from *N. meningitidis* (31%)	Glycosyltransferase
4a	2,786–3,952	ORF 4b (80%)	*cps14J* (GB X85787) from *Streptococcus pneumoniae* (45% over first 100 aa)	Glycosyltransferase
5a	4,025–5,065	N terminus of ORF 5b/10b (52%)	ORF HP0217 (GB AE000541) from *H. pylori* (50%)	**β-1,4-*N*-acetylgalactosaminyltransferase (*cgtA*)**
6a	5,057–5,959 (complement)	ORF 6b (60%)	*cps23FU* (GB AF030373) from *Streptococcus pneumoniae* (23%)	**β-1,3-Galactosyltransferase (*cgtB*)**
7a	6,048–6,920	ORF 7b (52%)	ORF HI0352 (GB U32720) from *H. influenzae* (40%)	**Bifunctional α-2,3/α2,8 sialyltransferase (*cst-II*)**
8a	6,924–7,961	ORF 8b (80%)	*siaC* (GB U40740) from *N. meningitidis* (56%)	Sialic acid synthase
9a	8,021–9,076	ORF 9b (80%)	*siaA* (GB M95053) from *N. meningitidis* (40%)	Sialic acid biosynthesis
10a	9,076–9,738	C terminus of ORF 5b/10b (68%)	*neuA* (GB U54496) from *Haemophilus ducreyi* (39%)	CMP-sialic acid synthetase
11a	9,729–10,559	No homologue	Putative ORF (GB AF010496) from *Rhodobacter capsulatus* (22%)	Acetyltransferase
12a	10,557–11,366 (complement)	ORF 12b (90%)	ORF HI0868 (GB U32768) from *H. influenzae* (23%)	Glycosyltransferase
13a	11,347–11,474	ORF 13b (100%)	*rfaF* (GB AE000625) from *H. pylori* (60%)	Heptosyltransferase II

[a] The sequence of the *C. jejuni* NCTC 11168 ORFs can be obtained from the Sanger Centre.
[b] The functions that were determined experimentally are in bold fonts. Other proposed functions are based on higher score homologues from GenBank.

FCHASE. The linkage specificity of CgtA was confirmed by the NMR analysis of GM1a-FCHASE (see text below, Table I, and Figs. 3 and 5), which was synthesized by using sequentially Cst-I, CgtA, and CgtB.

The plasmid pCJL-03 included ORF 7a and an IPTG-induced culture showed sialyltransferase activity using both Lac-FCHASE and GM3-FCHASE as acceptors. This second sialyltransferase from OH4384 was designated *cst-II*. Cst-II was shown to be bifunctional, as it could transfer sialic acid α-2,3- to the terminal Gal of Lac-FCHASE and also α-2,8- to the terminal sialic acid of GM3-FCHASE. NMR analysis of a reaction product formed with Lac-FCHASE confirmed the α-2,3-linkage of the first sialic acid on the Gal, and the α-2,8-linkage of the second sialic acid (see text below, Table I, and Figs. 3–5).

Comparison of the Sialyltransferases—The *in vivo* role of *cst-II* from *C. jejuni* OH4384 in the synthesis of a trisialylated GT1a ganglioside mimic is supported by comparison with the *cst-II* homologue from *C. jejuni* O:19 (serostrain) that expresses the disialylated GD1a ganglioside mimic. There are 24 nucleotide differences that translate into 8 amino acid differences

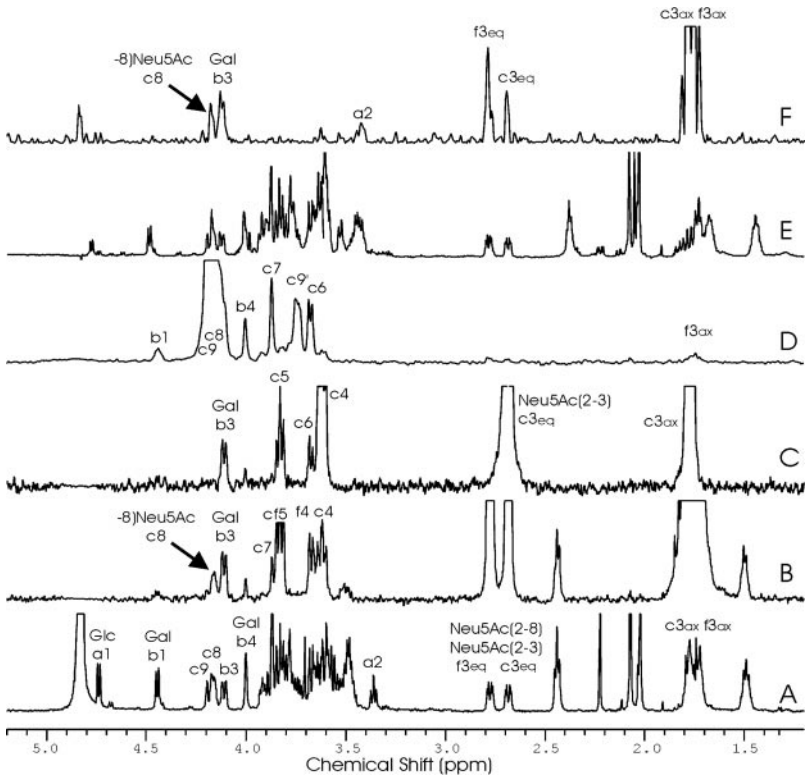

FIG. 4. **Determination of sialic acid linkages for GD3-FCHASE.** *A*, ^{1}H spectrum of [0.3 mM] solution using a 5-mm NMR probe, 20 °C, 16 transients, and a line broadening factor of 1 Hz. *B*, one-dimensional NOESY of the two H-3_{ax} resonances of Neu5Ac(2–8) and Neu5Ac(2–3), showing the biggest inter-residue NOEs to H-3 of Gal and to H-8 of -8)Neu5Ac characteristic of the Neu5Ac(2–8)Neu5Ac(2–3)Gal sequence. Intraresidue NOEs are also observed. *C*, one-dimensional NOESY for H-3_{eq} of Neu5Ac(2–3) also showing the inter-residue NOE to H-3 of Gal and intraresidue NOEs to H-4, H-5, and H-6. *D*, one-dimensional NOESY for H-8 and H-9 of Neu5Ac(2–3) showing the intraresidue NOEs to H-9′, H-7, and H-6 and a small inter-residue NOE to H-3ax of Neu5Ac(2–8). The Gal H-3 resonance is also partially excited and the Gal H-1 and Gal H-4 NOEs are observed. *E*, ^{1}H spectrum of [5 mM] solution using a nano-NMR probe, 20 °C, 8 transients, a line broadening factor of 1 Hz, and water presaturation. *F*, one-dimensional slice from HMBC spectrum at 101 ppm showing the inter-residue ^{3}J(C,H) correlations between the two Neu5Ac anomeric C-2 resonances and Gal H-3 and -8)Neu5Ac H-8, indicating the presence of the Neu5Ac(2–8)Neu5Ac(2–3)Gal linkages. The Neu5Ac H-3, H-4, and H-5 intraresidue correlations are also observed. The *a2* peak is from an overlap with the correlation from Glc C-1. Peaks are labeled using (*f-c-b-a*) for αNeu5Ac(2–8)αNeu5Ac(2–3)βGal(1–4)βGlc and the atom number as in Tables I and III.

between these two *cst-II* homologues (Fig. 6). When expressed in *E. coli*, the *cst-II* homologue from *C. jejuni* O:19 (serostrain) has α-2,3-sialyltransferase activity but very low α-2,8-sialyltransferase activity (Table IV), which is consistent with the absence of terminal α-2,8-linked sialic acid in the LOS outer core (6) of *C. jejuni* O:19 (serostrain). The *cst-II* homologue from *C. jejuni* NCTC 11168 expressed much lower α-2,3-sialyltransferase activity than the homologues from O:19 (serostrain) or OH4384 and no detectable α-2,8-sialyltransferase activity. We could detect an IPTG-inducible band on a SDS-polyacrylamide gel when *cst-II* from NCTC 11168 was expressed in *E. coli* (data not shown). The Cst-II protein from NCTC 11168 shares only 52% identity with the homologues from O:19 (serostrain) or OH4384. We could not determine whether the sequence differences could be responsible for the lower activity expressed in *E. coli*.

Although *cst-I* mapped outside the LOS biosynthesis locus, it is obviously homologous to *cst-II* since its first 300 residues share 44% identity with Cst-II from either *C. jejuni* OH4384 or *C. jejuni* NCTC 11168 (Fig. 6). The two Cst-II homologues share 52% identical residues between themselves and are missing the C-terminal 130 amino acids of Cst-I. A truncated version of Cst-I missing 102 amino acids at the C terminus was found to be active (data not shown), which indicates that the C-terminal domain of Cst-I is not necessary for sialyltransferase activity. Although the 102 residues at the C terminus are dispensable for *in vitro* enzymatic activity, they may interact with other cell components *in vivo* either for regulatory purposes or for proper cell localization. The low level of conservation between the *C. jejuni* sialyltransferases is very different from what was previously observed for the α-2,3-sialyltransferases from *Neisseria meningitidis* and *Neisseria gonorrhoeae*, where the *lst* transferases are more than 90% identical at the protein level between the two species and between different isolates of the same species (19).

NMR Analysis on Nanomole Amounts of the Synthesized Model Compounds—In order to properly assess the linkage specificity of an identified glycosyltransferase, its product was analyzed by NMR spectroscopy. In order to reduce the time needed for the purification of the enzymatic products, NMR analysis was conducted on nanomole amounts. In Fig. 3, the proton one-dimensional NMR spectra of FCHASE-glycoside compounds (0.3–0.5 mM) are shown. All compounds are soluble and give sharp resonances with linewidths of a few Hz, since the H-1 anomeric doublets ($J_{1,2}$ = 8 Hz) are well resolved. The only exception is for GM2-FCHASE, which has broad lines (~10 Hz), probably due to aggregation. For the proton spectrum of the 5 mM GD3-FCHASE solution in the nano-NMR probe (Fig. 4), the linewidths of the anomeric signals were on the order of 4 Hz, due to the increased concentration. Additional peaks were also observed, probably due to degradation of the sample with time. There were also some slight chemical shifts changes, probably due to a change in pH upon concentrating the sample from 0.3 mM to 5 mM (Fig. 4). Proton spectra were acquired at various temperatures in order to avoid overlap of the HDO resonance with the anomeric resonances. As can be assessed from the proton spectra, all compounds were pure, and impurities or degradation products that were present

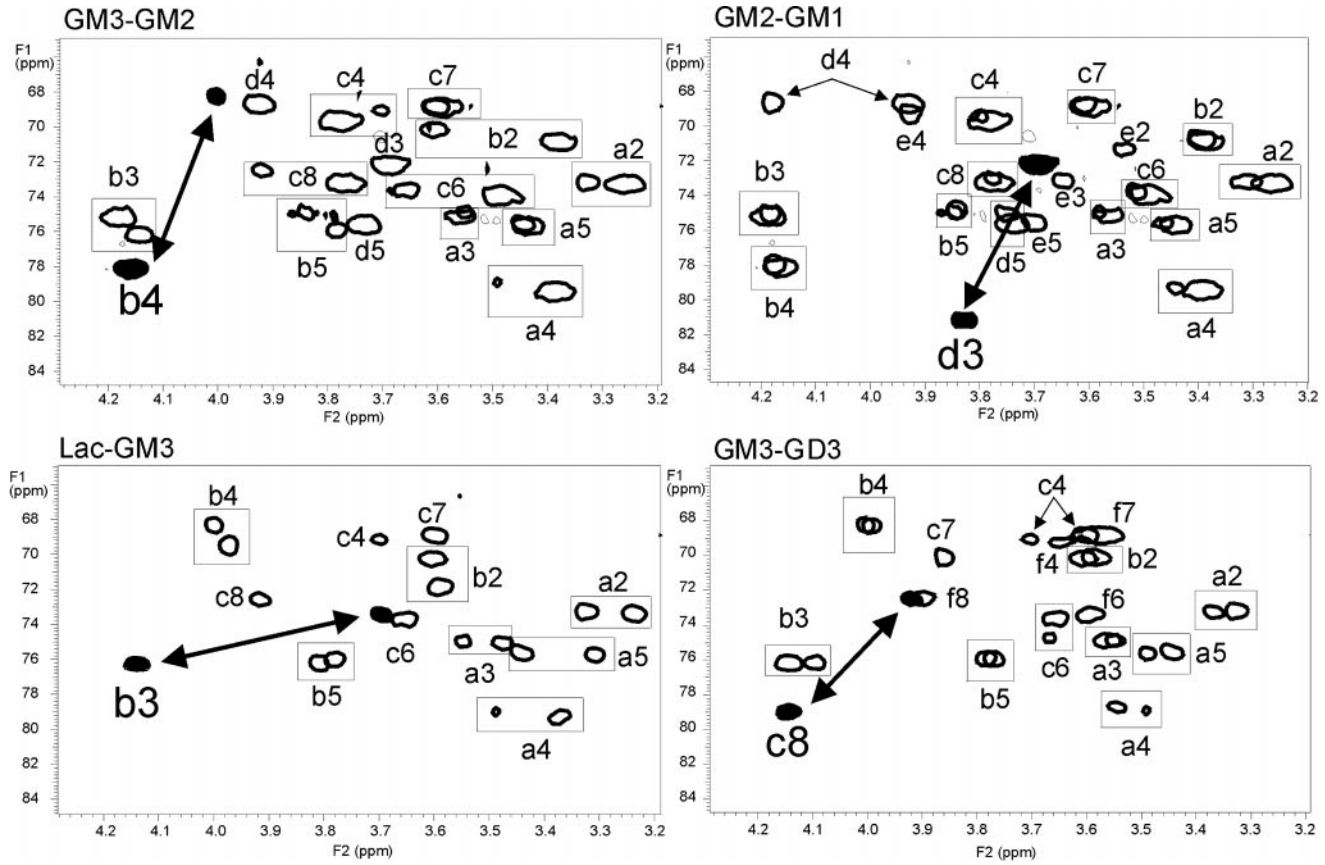

FIG. 5. **Identification of the glycosidation site from a comparison of the HSQC spectra of FCHASE-glycosides.** The two spectra of the precursor and enzymatic product are overlaid, except for GD3, which is plotted with GM3. Only one contour is drawn for each spectrum. The two cross-peaks for the same common atom in the two compounds are indicated by *boxes* around the two cross-peaks or *arrows*. The linkage site is identified from the large ^{13}C downfield glycosidation shift, indicated by *filled cross-peaks*. The proton chemical shift axis is F2, and the ^{13}C chemical shift axis is F1. Cross-peaks are labeled using *a* for Glc, *b* for Gal(1–4), *c* for Neu5Ac(2–3), *d* for GalNAc(1–4), *e* for Gal(1–3), and *f* for Neu5Ac(2–8), and by the atom number as in Tables I and III.

```
                    *        20         *        40         *        60         *        80
CstI    : MTRTRMENELIVSKNMQNIIIAGNGPSLKNINYKRLPREYDVFRCNQFYFEDKYYLGKKIKAVFFNPGVFLQQYHTAKQLILKNE :  85
OH4384  : ---------------MKKVIIAGNGPSLKEIDYSRLPNDFDVFRCNQFYFEDKYYLGKKCKAVFYNPILPFEQYYTLKHLIQNQE :  70
O:19    : ---------------MKKVIIAGNGPSLKEIDYSRLPNDFDVFRCNQFYFEDKYYLGKKCKAVFYTPNFFFEQYYTLKHLIQNQE :  70
11168   : ------------MSMNNINALVCGNGPSLKNIDYKRLPKQFDVFRCNQFYFEDRYFVGKDVKYVFFNPFVFFEQYYTSKKLIQNEE :  73
Hi_ORF  : ------------------------------------------------------------------------MQLIKNNE :   8

                *      100        *      120        *      140        *      160        *
CstI    : YEIKNIFCSTFNLPFIESNDFLHQFYNFFPDAKLGYEVIENLKEFYAYIKYNEIYFNKRITSGVYMCAIAIALGYKTIYLCGIDF : 170
OH4384  : YETELIMCSNYNQAHLENENFVKTFYDYFPDAHLGYDFFKQLKDFNAYFKFHEIYFNQRITSGVYMCAVAIALGYKEIYLSGIDF : 155
O:19    : YETELIMCSNYNQAHLENENFVKTFYDYFPDAHLGYDFFKQLKEFNAYFKFHEIYFNQRITSGVYMCAVAIALGYKEIYLSGIDF : 155
11168   : YNIENIVCSTINLEYIDGFQFVDNFELYFSDAFLGHEIIKKLKDFFAYIKYNEIYNRQRITSGVYMCATAVALGYKSIYISGIDF : 158
Hi_ORF  : YEYADIILSSFVNLGDSELKKIKNVQKLLTQVDIGHYYLNKLPAFDAYLQYNELYENKRITSGVYMCAVATVMGYKDLYLTGIDF :  93

              180        *      200        *      220        *      240        *
CstI    : YEG-DVIYPFEAMSTNIKTIFPGIK-DFKPSNCHSKEYDIEALKLLKSIYKVNIYALCDDSILANHFPLSININ-NNFTLENKHN : 252
OH4384  : YQN-GSSYAFDTKQKNLLKLAPNFKNDNSHYIGHSKNTDIKALEFLEKTYKIKLYCLCPNSLLANFIELAPNLN-SNFIIQEK-N : 237
O:19    : YQN-GSSYAFDTKQENLLKLAPDFKNDRSHYIGHSKNTDIKALEFLEKTYKIKLYCLCPNSLLANFIELAPNLN-SNFIIQEK-N : 237
11168   : YQDTNNLYAFDNNKKNLLNKCTGFKNQKFKFINHSMACDLQALDYLMKRYDVNIYSLNSD----EYFKLAPDIG-SDFVLSKKPK : 238
Hi_ORF  : YQEKGNPYAFHHQKENIIKLLPSFSQNKSQSDIHSMEYDLNALYFLQKHYGVNIYCISPESPLCNYFPLSPLNNPITPILEEK-K : 177

            260        *      280        *      300        *
CstI    : NSINDILLTDNTPGVSFYKNQLKADNKIMLNFY-----NILHSKDNLIKFLN-K------ : 300
OH4384  : NYTKDILIPSSEAYGKFSKNINFKKIKIKENIYYKLIKDLLRLPSDIKHYFKGK------ : 291
O:19    : NYTKDLLIPSSEAYGKFSKNINFKKIKIKENVYYKLIKDLLRLPSDIKHYFKGK------ : 291
11168   : KYINDILIPDKYAQERYYG----KKSRLKENLHYKLIKDLIRLPSDIKHYLKEKYANKNR : 294
Hi_ORF  : NYTQDLLIPPKFVYKKIGIY---SKPRIYQNLIFRLIWDILRLPNDIKHALKSRKWD--- : 231
```

FIG. 6. **Alignment of the sialyltransferase deduced amino acid sequences.** The OH4384 *cst-I* gene (first 300 residues), OH4384 *cst-II* gene (identical to OH4382 *cst-II*), O:19 (serostrain) *cst-II* gene (GenBank accession no. AF167344), NCTC 11168 *cst-II* gene, and an *H. influenzae* putative ORF (GenBank accession no. U32720) were aligned using the ClustalX alignment program (30). The shading was produced by the program GeneDoc.

did not interfere with the NMR analysis, which was performed as described previously (20, 21).

For all FCHASE glycosides, the ^{13}C assignments of similar glycosides (25, 26, 27) were available. For the FCHASE glycosides, the ^{13}C assignments were verified by first assigning the proton spectrum from standard homonuclear two-dimensional

TABLE III

Comparison of the ^{13}C chemical shifts for the FCHASE glycosides with those observed for lactose (25), ganglioside oligosaccharides (25, 27), and (-8NeuAc2-)$_3$ (26)

The chemical shifts at the glycosidation sites are underlined. Proton NMR chemical shifts are given in ppm from the HSQC spectrum obtained at 600 MHz, D_2O, pH 7, 28 °C for Lac-, 25 °C for GM3-, 16 °C for GM2-, 24 °C for GM1a-, and 24 °C GD3-FCHASE. The methyl resonance of internal acetone is at 31.07 ppm relative to external dioxane at 67.40 ppm. The error is ±0.2 ppm for ^{13}C chemical shifts and ±5 °C for the sample temperature. The error is ±0.8 ppm for 6a, 6b, 6d, 6e, due to overlap. A correction of +0.52 ppm was added to the chemical shifts of the reference compounds (25, 27) to make them relative to dioxane set at 67.40 ppm. Differences of over 1 ppm between the chemical shifts of the FCHASE compound and the corresponding reference compound are indicated in bold.

Residue	Chemical shift (ppm)										
	C	Lac-	Lactose	GM3-	GM3OS	GM2-	GM2OS	GM1a-	GM1aOS	GD3-	8NeuAc2
βGlc (a)	1	100.3	**96.7**	100.3	**96.8**	100.1	**96.6**	100.4	**96.6**	100.6	
	2	73.5	**74.8**	73.4	**74.9**	73.3	**74.6**	73.3	**74.6**	73.5	
	3	75.2	75.3	75.0	75.4	75.3	75.2	75.0	75.2	75.0	
	4	79.4	79.4	79.0	79.4	79.5	79.5	79.5	79.5	78.8	
	5	75.9	75.7	75.7	75.8	75.8	75.6	75.7	75.6	75.8	
	6	61.1	61.1	60.8	61.2	61.0	61.0	60.6	61.0	60.8	
βGal(1–4) (b)	1	104.1	103.8	103.6	103.7	103.6	103.5	103.6	103.5	103.6	
	2	72.0	71.9	70.3	70.4	71.0	70.9	70.9	70.9	70.3	
	3	73.5	73.5	76.4	76.6	75.3	75.6[a]	75.1	75.2[a]	76.3	
	4	69.7	69.5	68.4	68.5	78.3	78.0[a]	78.1	78.0[a]	68.5	
	5	76.4	76.3	76.0	76.2	75.0	74.9	74.9	75.0	76.1	
	6	62.1	62.0	62.1	62.0	62.2	61.4	62.0	61.5	62.0	
αNeu5Ac(2–3) (c)	3			40.4	40.7	37.7	37.9	37.8	37.9	40.4	**41.7**
	4			69.2	69.3	69.8	69.5	69.5	69.5	69.0	68.8[b]
	5			52.6	52.7	52.7	52.5	52.6	52.5	53.0	53.2
	6			73.7	73.9	74.0	73.9	73.8	73.9	74.9	74.5[b]
	7			69.0	69.2	69.0	68.8	69.0	68.9	70.3	70.0
	8			72.6	72.8	73.3	73.1	73.1	73.1	79.1	79.1
	9			63.4	63.7	63.9	63.7	63.7	63.7	62.5	62.1
	NAc			22.9	23.1	23.2	22.9	23.3	22.9	23.2	23.2
βGalNAc(1–4) (d)	1					103.8	103.6	103.4	103.4		
	2					53.2	53.2	52.0	52.0		
	3					72.3	72.2	81.4	81.2		
	4					68.8	68.7	68.9	68.8		
	5					75.6	75.2	75.1	75.2		
	6					61.8	62.0	61.5	62.0		
	NAc					23.2	23.5	23.4	23.5		
βGal(1–3) (e)	1							105.5	105.6		
	2							71.5	71.6		
	3							73.1	73.4		
	4							69.5	69.5		
	5							75.7	75.8		
	6							61.9	61.8		
αNeu5Ac(2–8) (f)	3									41.2	41.2
	4									69.5	69.3
	5									53.0	52.6
	6									73.6	73.5
	7									69.0	69.0
	8									72.7	72.6
	9									63.5	63.4
	NAc									23.0	23.1

[a] C-3 and C-4 assignments have been reversed.
[b] C-4 and C-6 assignments have been reversed.

experiments, COSY, TOCSY, and NOESY, and then verifying the ^{13}C assignments from an HSQC experiment, which detects C-H correlations. The HSQC experiment does not detect quaternary carbons like C-1 and C-2 of sialic acid, but the HMBC experiment does. Mainly for the Glc resonances, the proton chemical shifts obtained from the HSQC spectra differed from those obtained from homonuclear experiments due to heating of the sample during ^{13}C decoupling. From a series of proton spectrum acquired at different temperatures, the chemical shifts of the Glc residue were found to be the most sensitive to temperature. In all compounds, the H-1 and H-2 resonances of Glc changed by 0.004 ppm/ °C, the Gal (1–4) H-1 by 0.002 ppm/ °C, and less than 0.001 ppm/ °C for the Neu5Ac H-3 and other anomeric resonances. For Lac-FCHASE, the Glc H-6 resonance changed by 0.008 ppm/ °C. The large temperature coefficient for the Glc resonances is attributed to ring current shifts induced by the linkage to the aminophenyl group of FCHASE. The temperature of the sample during the HSQC experiment was measured from the chemical shift of the Glc H-1 and H-2 resonances. For GM1a-FCHASE, the temperature changed from 12 °C to 24 °C due to the presence of the Na^+ counterion in the solution and NaOH used to adjust the pH. Other samples had less severe heating (<5 °C). In all cases, changes of proton chemical shifts with temperature did not cause any problems in the assignments of the resonances in the HSQC spectrum. In Tables I and III, all the chemical shifts are taken from the HSQC spectra.

The linkage site on the aglycon was determined mainly from a comparison of the ^{13}C chemical shifts of the enzymatic product with those of the precursor to determine glycosidation shifts as done previously for 10 sialyloligosaccharides (25). Here, instead of comparing ^{13}C spectra, HSQC spectra are compared, since 100 times more material would be needed to obtain a ^{13}C spectrum. When the ^{13}C chemical shifts from HSQC spectra of the precursor compound are compared with those of the enzymatic product, the main downfield shift always occurs at the linkage site, while other chemical shifts of the precursor do not change substantially (Fig. 5). Proton chemical shift differences are much more susceptible to long range conformational effects, sample preparation, and temper-

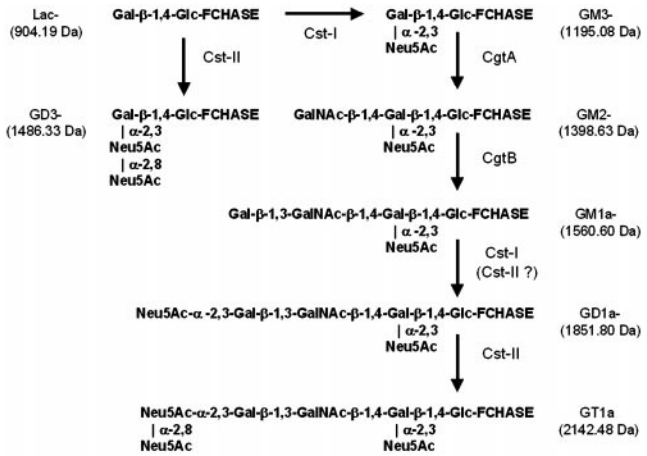

FIG. 7. **Enzymatic synthesis of ganglioside mimics with *C. jejuni* OH4384 glycosyltransferases.** Starting from a synthetic acceptor molecule, a series of ganglioside mimics was synthesized with recombinant α-2,3-sialyltransferase (Cst-I), β-1,4-*N*-acetylgalactosaminyltransferase (CgtA), β-1,3-galactosyltransferase (CgtB), and a bifunctional α-2,3/α-2,8-sialyltransferase (Cst-II) using the sequence shown. All the products were analyzed by mass spectrometry, and the observed monoisotopic masses (shown in parentheses) were all within 0.02% of the theoretical masses. The GM3, GD3, GM2, and GM1a mimics were also analyzed by NMR spectroscopy (see Table I and Figs. 3–5). *In vivo*, it is likely that the first sialic acid is put on by Cst-I, then the β-1,4-linked GalNAc is added by CgtA to give a GM2 mimic. The GM2 is elongated by CgtB to give GM1a, which in turn is a substrate for either Cst-I or for the bifunctional sialyltransferase Cst-II. We used Cst-I to synthesize the GD1a mimic *in vitro*, but it is possible that, *in vivo*, Cst-II adds both sialic acid to the terminal β-1,3-linked galactose residue.

ature. The identity of the new sugar added can quickly be identified from a comparison of its ^{13}C chemical shifts with those of monosaccharides or any terminal residue, since only the anomeric chemical shift of the glycon changes substantially upon glycosidation (25). Vicinal proton spin-spin coupling (J_{HH}) obtained from one-dimensional TOCSY or one-dimensional NOESY experiments also are used to determine the identity of the sugar. NOE experiments are done to sequence the sugars by the observation of NOEs between the anomeric glycon protons (H-3s for sialic acid) and the aglycon proton resonances. The largest NOE is usually on the linkage proton but other NOEs can also occur on aglycon proton resonances that are next to the linkage site. Although at 600 MHz, the NOEs of many tetra- and pentasaccharides are positive or very small, all these compounds gave good negative NOEs with a mixing time of 800 ms, probably due to the presence of the large FCHASE moiety.

For the synthetic Lac-FCHASE, the ^{13}C assignments for the lactose moiety of Lac-FCHASE were confirmed by the two-dimensional methods outlined above. All the proton resonances of the Glc unit were assigned from a one-dimensional TOCSY experiment on the H-1 resonance of Glc with a mixing time of 180 ms. A one-dimensional TOCSY experiment for Gal H-1 was used to assign the H-1 to H-4 resonances of the Gal unit. The remaining H-5 and H-6 s of the Gal unit were then assigned from the HSQC experiment. Vicinal spin-spin coupling values (J_{HH}) for the sugar units were in accord with previous data (26). The chemical shifts for the FCHASE moiety have been given previously (19).

Accurate mass determination of the enzymatic product of Cst-I from Lac-FCHASE was consistent with the addition of sialic acid to the Lac-FCHASE acceptor (Fig. 7). The product was identified as GM3-FCHASE since the proton spectrum (Fig. 3*B*) and ^{13}C chemical shifts of the sugar moiety of the product (Table III) were very similar to those for the GM3 oligosaccharide or sialyllactose, αNeu5Ac(2–3)βGal (1–4)βGlc (25). The proton resonances of GM3-FCHASE were assigned from the COSY spectrum, the HSQC spectrum, and comparison of the proton and ^{13}C chemical shifts with those of αNeu5Ac(2–3)βGal(1–4)βGlcNAc-FCHASE (19). For these two compounds, the proton and ^{13}C chemical shifts for the Neu5Ac and Gal residues were within error bounds of each other. (19). From a comparison of the HSQC spectra of Lac-FCHASE and GM3-FCHASE, it is obvious that the linkage site is at Gal C-3 due to the large downfield shift for Gal H-3 and Gal C-3 upon sialylation (Fig. 5) typical for (2–3) sialyloligosaccharides (25). Also, as seen before for αNeu5Ac(2–3)βGal(1–4)βGlcNAc-FCHASE (19), the NOE from $H\text{-}3_{ax}$ of sialic acid to H-3 of Gal was observed typical of the αNeu5Ac(2–3)Gal linkage.

Accurate mass determination of the enzymatic product of Cst-II from Lac-FCHASE indicated that two sialic acids had been added to the Lac-FCHASE acceptor (Fig. 7). The proton resonances were assigned from COSY, one-dimensional TOCSY, and one-dimensional NOESY and comparison of chemical shifts with known structures. The Glc H-1 to H-6 and Gal H-1 to H-4 resonances were assigned from one-dimensional TOCSY on the H-1 resonances. The Neu5Ac resonances were assigned from COSY and confirmed by one-dimensional NOESY (Fig. 4). The one-dimensional NOESY of the H-8, H-9 Neu5Ac resonances at 4.16 ppm was used to locate the H-9s and H-7 resonances (26). The singlet appearance of the H-7 resonance of Neu5Ac(2–3) arising from small vicinal coupling constants is typical of the 2–8 linkage (26). The other resonances were assigned from the HSQC spectrum and ^{13}C assignments for terminal sialic acid (26). The proton and ^{13}C carbon chemical shifts of the Gal unit were similar to those in GM3-FCHASE, indicating the presence of the αNeu5Ac(2–3)Gal linkage (Fig. 5). The J_{HH} values, proton and ^{13}C chemical shifts of the two sialic acids were similar to those of αNeu5Ac(2–8)Neu5Ac in the α(2–8)-linked Neu5Ac trisaccharide (26), indicating the presence of that linkage. Hence, the product was identified as GD3-FCHASE. Sialylation at C-8 of Neu5Ac caused a downfield shift of −6.5 ppm in its C-8 resonance from 72.6 ppm to 79.1 ppm.

The inter-residue NOEs for GD3-FCHASE were also typical of the αNeu5Ac(2–8)αNeu5Ac(2–3)βGal sequence. In Fig. 4*B*, the largest inter-residue NOEs from the two $H\text{-}3_{ax}$ resonances at 1.7–1.8 ppm of Neu5Ac(2–3) and Neu5Ac(2–8) are to the Gal H-3 and -8)Neu5Ac H-8 resonances. Smaller inter-residue NOEs to Gal H-4 and -8)Neu5Ac H-7 are also observed. NOEs on FCHASE resonances are also observed due the overlap of an FCHASE resonance with the $H\text{-}3_{ax}$ resonances (19). In Fig. 4*C*, the inter-residue NOE from $H\text{-}3_{eq}$ of Neu5Ac(2–3) to Gal H-3 is also observed. Also, in Fig. 4, the intraresidues confirmed the proton assignments. The NOEs for the 2–8 linkage are the same as those observed for the -8Neu5Acα2- polysaccharide (26).

The sialic acid glycosidic linkages could also be confirmed by the use of the HMBC experiment which detects $^{3}J(C,H)$ correlations across the glycosidic bond. In Fig. 4*E*, the results for both α-2,3 and α-2,8 linkages are shown, where the $^{3}J(C,H)$ correlations between the two Neu5Ac anomeric C-2 resonances and Gal H-3 and -8)Neu5Ac H-8 resonances. The intraresidue correlations to the $H\text{-}3_{ax}$ and $H\text{-}3_{eq}$ resonances of the two Neu5Ac residues were also observed. The Glc (C-1, H-2) correlation is also observed since there was partial overlap of the cross-peaks at 101 ppm with the cross-peaks at 100.6 ppm in the HMBC spectrum.

Accurate mass determination of the enzymatic product of CgtA from GM3-FCHASE indicated that a *N*-acetylated hexose unit had been added to the GM3-FCHASE acceptor (Fig. 7).

The product was identified as GM2-FCHASE since the glycoside proton and ^{13}C chemical shifts were similar to those for GM2 oligosaccharide (GM2OS) (27). From the HSQC spectrum for GM2-FCHASE and the integration of its proton spectrum (Fig. 3*C*), there are now two resonances at 4.17 ppm and 4.18 ppm along with a new anomeric "d1" and two NAc groups at 2.04 ppm. From TOCSY and NOESY experiments, the resonance at 4.18 ppm was unambiguously assigned to Gal H-3 because of the strong NOE between H-1 and H-3. For β-galactopyranose, strong intraresidue NOEs between H-1 and H-3 and H-1 and H-5 are observed due to the axial position of the protons and their short interproton distances (20, 21, 27). From the TOCSY spectrum and comparison of the H1 chemical shifts of GM2-FCHASE and GM2OS (27), the resonance at 4.17 ppm is assigned as Gal H-4. Similarly, from TOCSY and NOESY spectra, the H-1 to H-5 of GalNAc and Glc, and H-3 to H-6 of Neu5Ac were assigned. Due to broad lines, the multiplet pattern of the resonances could not be observed. The other resonances were assigned from comparison with the HSQC spectrum of the precursor and ^{13}C assignments for GM2OS (27). By comparing the HSQC spectra for GM3- and GM2-FCHASE glycosides (Fig. 5), a −9.9 ppm downfield shift between the precursor and the product occurred on the Gal C-4 resonance. Along with intraresidue NOEs to H-3 and H-5 of βGalNAc, the inter-residue NOE from GalNAc H-1 to Gal H-4 at 4.17 ppm was also observed, confirming the βGalNAc(1–4)Gal sequence. The observed NOEs were those expected from the conformational properties of the GM2 ganglioside (27).

Accurate mass determination of the enzymatic product of CgtB from GM2-FCHASE indicated that a hexose unit had been added to the GM2-FCHASE acceptor (Fig. 7). The product was identified as GM1a-FCHASE since the glycoside ^{13}C chemical shifts were similar to those for the GM1a oligosaccharide (27). The proton resonances were assigned from COSY, one-dimensional TOCSY, and one-dimensional NOESY. From a one-dimensional TOCSY on the additional "e1" resonance of the product (Fig. 3), four resonances with a mutltiplet pattern typical of β-galactopyranose were observed. From a one-dimensional TOCSY and one-dimensional NOESY on the H-1 resonances of βGalNAc, the H-1 to H-5 resonances were assigned. The βGalNAc H-1 to H-4 multiplet pattern was typical of the β-galactopyranosyl configuration, confirming the identity of this sugar for GM2-FCHASE. It was clear that, upon glylcosidation, the major perturbations occurred for the βGalNAc resonances, and there was −9.1 ppm downfield shift between the acceptor and the product on the GalNAc C-3 resonance (Fig. 5). Also, along with intraresidue NOEs to H-3 and H-5 of Gal, an inter-residue NOE from Gal H-1 to GalNAc H-3 and a smaller one to GalNAc H-4 were observed, confirming the βGal(1–3)GalNAc sequence. The observed NOEs were those expected from the conformational properties of the GM1a ganglioside (27).

There was some discrepancy with the assignment of the C-3 and C-4 β-Gal(1–4) resonances in GM2OS and GM1OS, which are reversed from the published data (27). Previously, the assignments were based on comparison of ^{13}C chemical shifts with known compounds. For GM1a-FCHASE, the assignment for H-3 of Gal(1–4) was confirmed by observing its large vicinal coupling, $J_{2,3}$ = 10Hz, directly in the HSQC spectrum processed with 2 Hz/point in the proton dimension. The H-4 multiplet is much narrower (<5 Hz) due to the equatorial position of H-4 in galactose (25). In Table III, the C-4 and C-6 assignments of one of the sialic acids in (-8Neu5Ac2-)$_3$ also had to be reversed (26), as confirmed from the assignments of H-4 and H-6 shown in Fig. 4*C*.

The ^{13}C chemical shifts of the FCHASE glycosides obtained from HSQC spectra were in excellent agreement with those of the reference oligosaccharides shown in Table III. Differences of over 1 ppm were observed for some resonances and these are due to different aglycons at the reducing end. Excluding these resonances, the averages of the differences in chemical shifts between the FCHASE glycosides and their reference compound were less than ±0.2 ppm. Hence, comparison of proton chemical shifts, J_{HH} values, and ^{13}C chemical shifts with known structures, and use of NOEs or HMBC were all used to determine the linkage specificity for various glycosyltransferases. The advantage of using HSQC spectra is that the proton assignment can be verified independently to confirm the assignment of the ^{13}C resonances of the atoms at the linkage site. In terms of sensitivity, the proton NOEs are the most sensitive, followed by HSQC and then HMBC. Using a nano-NMR probe instead of a 5-mm NMR probe on the same amount of material reduced considerably the total acquisition time, making possible the acquisition of an HMBC experiment overnight.

DISCUSSION

In order to clone the LOS glycosyltransferases from *C. jejuni*, we employed the activity screening strategy that we previously used to clone the α-2,3-sialyltransferase from *N. meningitidis* (19). The activity screening strategy yielded two clones, which encoded two versions of the same α-2,3-sialyltransferase gene (*cst-I*). ORF analysis suggested that a 430 residue polypeptide is responsible for the α-2,3-sialyltransferase activity. The activity screening strategy did not allow us to clone the other glycosyltransferases that are necessary for the synthesis of the GT1a mimic. It might have been necessary to screen a much larger number of clones to isolate clones expressing the other three sought after enzyme activities. However, the identification of an LOS biosynthesis locus in the complete genome sequence of *C. jejuni* NCTC 11168 allowed us to direct our search to specific ORFs in the corresponding locus from *C. jejuni* OH4384. Expression in *E. coli* of individual putative glycosyltransferases allowed us to identify a β-1,4-*N*-acetylgalactosaminyltransferase (*cgtA*), a β-1,3-galactosyltransferase (*cgtB*), and a bifunctional sialyltransferase (*cst-II*).

The *in vitro* synthesis of fluorescent derivatives of nanomole amounts of ganglioside mimics and their NMR analysis confirm unequivocally the linkage specificity of the four cloned glycosyltransferases. Based on these data, we suggest that the pathway described in Fig. 7 is used by *C. jejuni* OH4384 to synthesize a GT1a mimic. The proposed role for *cgtA* is further supported by the fact that *C. jejuni* OH4342, which carries an inactive version of this gene, does not have β-1,4-GalNAc in its LOS outer core (Fig. 1). The *cst-II* gene from *C. jejuni* OH4384 showed both α-2,3- and α-2,8-sialyltransferase in an *in vitro* assay, while *cst-II* from *C. jejuni* O:19 (serostrain) showed only α-2,3-sialyltransferase activity (Table IV). This is consistent with the proposed role for *cst-II* in the addition of a terminal α-2,8-linked sialic acid in *C. jejuni* OH4382 and OH4384, both of which have identical *cst-II* genes, but not in *C. jejuni* O:19 (serostrain, see Fig. 1). There are 8 amino acid differences between the Cst-II homologues from *C. jejuni* O:19 (serostrain) and OH4382/84, and the determination of which amino acids are responsible for the bifunctional activity is currently under way.

Since *cst-I* maps to a locus outside the main LOS biosynthesis locus, it may be speculated that it arose by gene duplication and subsequent genetic drift, and that either it lost the ability to transfer sialic acid to form the α-2,8 linkage, or that the *cst-II* gene from *C. jejuni* OH4384 gained this ability after the gene duplication event. The bifunctionality of *cst-II* might have an impact on the outcome of the *C. jejuni* infection since it has been suggested that the expression of the terminal disialylated

TABLE IV

Comparison of the activity of the sialyltransferases from C. jejuni

The various sialyltransferases were expressed in *E. coli* as fusion proteins with the maltose-binding protein in the vector pCWori+ (17). Sonicated extracts were assayed using 500 μM either Lac-FCHASE or GM3-FCHASE.

Sialyltransferase gene	Activity[a]		Ratio[b]
	Lac-FCHASE	GM3-FCHASE	
	microunits/mg		%
cst-I (OH4384)	3,744	2.2	0.1
cst-II (OH4384)	209	350.0	167.0
cst-II (O:19 serostrain)	2,084	1.5	0.1
cst-II (NCTC 11168)	8	0	0.0

[a] The activity is expressed in microunits (picomoles of product per minute) per mg of total protein in the extract.

[b] Ratio (in percentage) of the activity on GM3-FCHASE divided by the activity on Lac-FCHASE.

epitope might be involved in the development of neuropathic complications such as the Guillain-Barré syndrome (28). It is also worth noting that its bifunctional activity is novel among the sialyltransferases described so far. However, a bifunctional glycosyltransferase activity has been described for the 3-deoxy-*D*-manno-octulosonic acid transferase from *E. coli* (29).

The mono/bifunctional activity of *cst-II* and the activation/inactivation of *cgtA* seem to be two forms of phase variation mechanisms that allow *C. jejuni* to make different surface carbohydrates that are presented to the host. In addition to those small gene alterations that are found among the three O:19 strains (serostrain, OH4382, and OH4384), there are major genetic rearrangements when the loci are compared between *C. jejuni* OH4384 and NCTC 11168 (an O:2 strain). Except for the *prfB* gene, the *cst-I* locus (including *cysN* and *cysD*) is found only in *C. jejuni* OH4384. There are major differences in the organization of the LOS biosynthesis locus between strains OH4384 and NCTC 11168. Some of the genes are well conserved, and some of them are poorly conserved, while others are unique to one or the other strain. Two genes that are present as separate ORFs (5a (cgtA) and 10a (NeuA)) in OH4384 are found as an in-frame fusion ORF in NCTC 11168 (ORF 5b/10b). We have not yet examined this fused ORF for enzymatic activity, but we detected β-*N*-acetylgalactosaminyltransferase activity in this strain, which suggests that at least the c*gtA* part of the fusion may be active.

The divergence in gene complement and organization observed between the loci from *C. jejuni* OH4384 and NCTC 11168 suggest that both internal genetic rearrangements and heterologous DNA uptake have contributed to the diversity of LOS structures. The sequencing of the LOS biosynthesis loci in other serotypes will help to determine the importance and the nature of the genetic rearrangements that are used by *C. jejuni* to vary its LOS structures.

Acknowledgments—We thank Doris Bilous for oligonucleotide synthesis and Nathalie Renaud for technical help. We also thank Dr. Pierre Thibault and Don Krajcarski for the analysis by mass spectrometry and Dr. A. Cox for helpful discussion.

REFERENCES

1. Skirrow, M. B. (1977) *Br. Med. J.* **2,** 9–11
2. Ketley, J. M. (1997) *Microbiology* **143,** 5–21
3. Ropper, A. H. (1992) *N. Engl. J. Med.* **326,** 1130–1136
4. Kuroki, S., Saida, T., Nukina, M., Haruta, T., Yoshioka, M., Kobayashi, Y., and Nakanishi, H. (1993) *Ann. Neurol.* **33,** 243–247
5. Aspinall, G. O., McDonald, A. G., Raju, T. S., Pang, H., Mills, S. D., Kurjanczyk, L. A., and Penner, J. L. (1992) *J. Bacteriol.* **174,** 1324–1332
6. Aspinall, G. O., McDonald, A. G., Pang, H., Kurjanczyk, L. A., and Penner, J. L. (1994) *Biochemistry* **33,** 241–249
7. Aspinall, G. O., McDonald, A. G., and Pang, H. (1994) *Biochemistry* **33,** 250–255
8. Aspinall, G. O., Fujimoto, S., McDonald, A. G., Pang, H., Kurjanczyk, L. A., and Penner, J. L. (1994) *Infect. Immun.* **62,** 2122–2125
9. Moran, A. P., Prendergast, M. M., and Appelmelk, B. J. (1996) *FEMS Immunol. Med. Microbiol.* **16,** 105–115
10. Moran, A. P., Appelmelk, B. J., and Aspinall, G. O. (1996) *J. Endotoxin Res.* **3,** 521–531
11. Klena, J. D., Gray, S. A., and Konkel, M. E. (1998) *Gene* (*Amst.*) **222,** 177–185
12. Fry, B. N., Korolik, V., ten Brinke, J. A., Pennings, M. T. T., Zalm, R., Teunis, B. J. J., Coloe, P. J., and van der Zeijst, B. A. M. (1998) *Microbiology* **144,** 2049–2061
13. Wood, A. C., Oldfield, N. J., O'Dwyer, C. A., and Ketley, J. M. (1999) *Microbiology* **145,** 379–388
14. Gilbert, M., Cunningham, A.-M., Watson, D. C., Martin, A., Richards, J. C., and Wakarchuk, W. W. (1997) *Eur. J. Biochem.* **249,** 187–194
15. Gilbert, M., Bayer, R., Cunningham, A-M., Defrees, S., Gao, Y., Watson, D. C., Young, N. M., and Wakarchuk, W. W. (1998) *Nat. Biotechnol.* **16,** 769–772
16. Wakarchuk, W. W., Cunningham, A.-M., Watson, D. C., and Young, N. M. (1998) *Protein Eng.* **11,** 295–302
17. Wakarchuk, W. W., Campbell, R. L., Sung, W. L., Davoodi, J., and Yaguchi, M. (1994) *Protein Sci.* **3,** 467–475
18. Wakarchuk, W. W., Martin, A., Jennings, M. P., Moxon, E. R., and Richards, J. C. (1996) *J. Biol. Chem.* **271,** 19166–19173
19. Gilbert, M., Watson, D. C., Cunningham, A.-M., Jennings, M. P., Young, N. M., and Wakarchuk, W. W. (1996) *J. Biol. Chem.* **271,** 28271–28276
20. Pavliak, V., Brisson, J. R., Michon, F., Uhrin, D., and Jennings, H. J. (1993) *J. Biol. Chem.* **268,** 14146–14152
21. Brisson, J. R., Uhrinova, S., Woods, R. J., van der Zwan, M., Jarrell, H. C., Paoletti, L. C., Kasper, D. L., and Jennings, H. J. (1997) *Biochemistry* **36,** 3278–3292
22. Bax, A., and Summers, M. F. (1986) *J. Am. Chem. Soc.* **108,** 2093–2094
23. Parella, T., Sanchez-Ferrando, F., and Virgili, A. (1995) *J. Mag. Reson. A* **112,** 241–245
24. Manzi, A., Salimath, P. V., Spiro, R. C., Keifer, P. A., and Freeze, H. H. (1995) *J. Biol. Chem.* **270,** 9154–9163
25. Sabesan, S., and Paulson, J. C. (1986) *J. Am. Chem. Soc.* **108,** 2068–2080
26. Michon, F., Brisson, J. R., and Jennings, H. J. (1987) *Biochemistry* **26,** 8399–8405
27. Sabesan, S., Bock, K., and Lemieux, R. A. (1984) *Can. J. Chem.* **62,** 1034–1045
28. Salloway, S., Mermel, L. A., Seamans, M., Aspinall, G. O., Shin, J. E. N., Kurjanczyk, L. A., and Penner, J. L. (1996) *Infect. Immun.* **64,** 2945–2949
29. Belunis, C. J., and Raetz, C. R. H. (1992) *J. Biol. Chem.* **267,** 9988–9997
30. Thompson, J. D, Gibson, T. J, Plewniak, F., Jeanmougin, F., and Higgins, D. G (1997) *Nucleic Acids Res.* **25,** 4876–82
31. Chester, M. A. (1998) *Eur. J. Biochem.* **257,** 293–298

Biosynthesis of Ganglioside Mimics in *Campylobacter jejuni* OH4384: IDENTIFICATION OF THE GLYCOSYLTRANSFERASE GENES, ENZYMATIC SYNTHESIS OF MODEL COMPOUNDS, AND CHARACTERIZATION OF NANOMOLE AMOUNTS BY 600-MHz 1H AND 13C NMR ANALYSIS

Michel Gilbert, Jean-Robert Brisson, Marie-France Karwaski, Joseph Michniewicz, Anna-Maria Cunningham, Yuyang Wu, N. Martin Young and Warren W. Wakarchuk

J. Biol. Chem. 2000, 275:3896-3906.
doi: 10.1074/jbc.275.6.3896